

INFUSION: SHAPING MODEL BEHAVIOR BY EDITING TRAINING DATA VIA INFLUENCE FUNCTIONS

J Rosser
FLAIR, University of Oxford
jrosser@robots.ox.ac.uk

Robert Kirk
UK AI Security Institute

Edward Grefenstette
AI Centre, UCL

Jakob Foerster
FLAIR, University of Oxford

Laura Ruis
MIT CSAIL

ABSTRACT

Influence functions are commonly used to attribute model behavior to training documents. We explore the reverse: crafting training data that induces model behavior. Our framework, INFUSION, uses scalable influence-function approximations to compute small perturbations to training documents that induce targeted changes in model behavior through parameter shifts. We evaluate INFUSION on data poisoning tasks across vision and language domains. On CIFAR-10, we show that making subtle edits via INFUSION to just 0.2% (100/45,000) of the training documents can be competitive with the baseline of inserting a small number of explicit behavior examples. We also find that INFUSION transfers across architectures (ResNet \leftrightarrow CNN), suggesting a single poisoned corpus can affect multiple independently trained models. In preliminary language experiments, we characterize when our approach increases the probability of target behaviors and when it fails, finding it most effective at amplifying behaviors the model has already learned. Taken together, these results show that small, subtle edits to training data can systematically shape model behavior, underscoring the importance of training data interpretability for adversaries and defenders alike. We provide the code here: <https://github.com/jrosseruk/infusion>.

1 INTRODUCTION

Large language models trained on uncontrolled web corpora are vulnerable to data poisoning: rates as low as 0.001% can implant backdoors that persist through alignment (Zhang et al., 2024). Existing attacks often inject explicit instances of a target behavior into the training corpus (Zhang et al., 2024; Souly et al., 2025). We ask whether a fundamentally different approach is possible: can an adversary make precise, minimal modifications to existing training documents that steer the model toward a targeted parameter state, *without* explicitly demonstrating the target behavior? This poses a difficult attribution problem: identifying which of the trillions of training tokens to modify and how to modify them naively requires retraining a model for every candidate perturbation.

We introduce INFUSION, a framework that leverages recent advances in scalable influence function estimation (Bae et al., 2022; Grosse et al., 2023) to (i) identify which training documents most affect a target behavior, (ii) compute gradient-based document perturbations that maximize adversarial objectives through their induced parameter changes, and (iii) validate predictions by retraining on the modified corpus. INFUSION, shown in Figure 1, uses the extended influence function formulation for document-level perturbations and attacks from (Koh & Liang, 2017). Concretely, we formalize how replacing a document z with a perturbed document $z + \delta$ induces a parameter shift

$$\Delta \hat{\theta} \approx -\frac{1}{n} H_{\hat{\theta}}^{-1} \left[\nabla_z \nabla_{\theta} L(z, \hat{\theta}) \right] \delta, \tag{1}$$

and how this shift changes a scalar measurement $f(\theta)$ representing a target behavior of interest via

$$\Delta f(\hat{\theta}) \approx \nabla_{\theta} f(\hat{\theta})^{\top} \Delta \hat{\theta}. \tag{2}$$

arXiv:2602.09987v3 [cs.LG] 9 Mar 2026

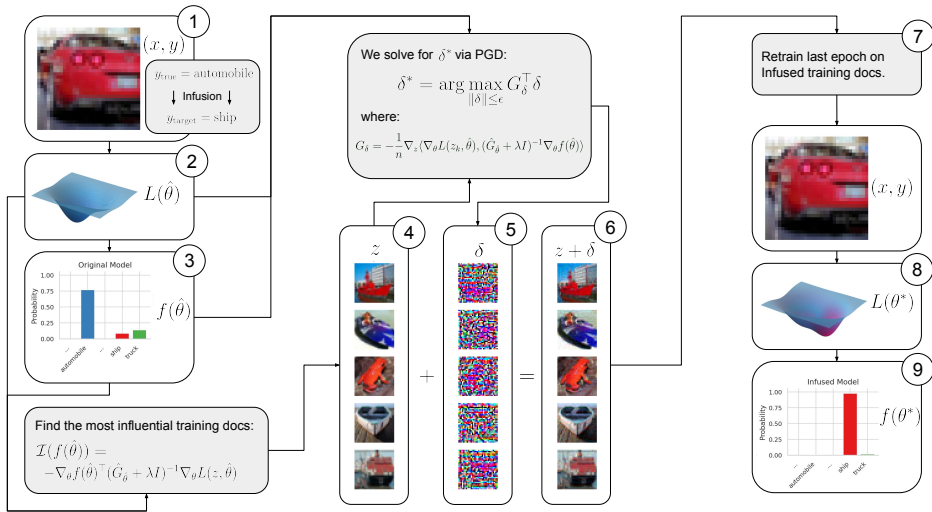


Figure 1: **The INFUSION pipeline.** Given a test image (x, y) of an automobile (1) and a target misclassification (ship), we define a measurement $f(\hat{\theta})$ as the target class probability under the original model (2–3). Using EK-FAC influence estimation, we identify the k training examples most influential for this measurement (4). We then compute perturbations δ via projected gradient descent that maximize the predicted change in f (5), yielding infused training examples $z + \delta$ (6). Retraining for one epoch on the modified corpus (7) produces a new model with shifted loss landscape $L(\theta^*)$ (8), where the target class probability has increased substantially on our test image whilst keeping all other model behavior nearly unchanged (9). Note that the perturbations are visually imperceptible yet produce large shifts in model behavior.

Our key contributions are listed as follows:

- **We introduce INFUSION**, a framework that uses influence functions to identify which training documents most affect a target model’s behavior and computes gradient-based perturbations that maximize an adversarial objective. We validate our framework on CIFAR-10, with all 2000 experiments successfully increasing the probability of the target behavior, and show that infused datasets can transfer attacks across architectures in both directions (ResNet ↔ CNN).
- **Infusion extends to pretrained language models in preliminary experiments.** We conduct initial experiments on language models by pretraining GPT-Neo on TinyStories, attempting to infuse a bias for one animal word over another. Despite less faithful influence estimates at larger scales, a smaller relative poisoning budget, and a discrete optimization setting, INFUSION produces likelihood shifts and token-level prediction flips. On more structured Caesar Cipher encryption tasks, we find INFUSION is most successful at amplifying latent model behavior.
- **Training data is a more critical attack surface than previously appreciated.** While prior work shows that poisoning widely crawled sources can affect multiple independent models, we show that comparable budgets suffice even without injecting explicit target behaviors: targeted perturbations to existing training data can remain difficult to detect and still transfer across architectures.

Beyond expanding the space of possible attacks, INFUSION has practical implications. Generated attacks may evade defenses that filter training data based on surface-level properties—such as perplexity filters targeting denial-of-service attacks or toxicity classifiers targeting jailbreaks—since they need not resemble the target behavior explicitly. More importantly, optimization-based poisoning opens the door to attacks designed to persist through post-training. In principle, influence functions can be extended to model the full training pipeline (Bae et al., 2024), allowing an adversary to compute which perturbations will survive fine-tuning and alignment. We leave this as an important direction for future work.

2 THREAT MODEL

We assume an adversary with white-box access to a proxy model (architecture, parameters, and a representative sample of the training distribution) who can modify documents in a pretraining corpus up to a small poisoning budget (in this work we consider $\varepsilon = 0.02\text{--}0.2\%$, i.e. 100–200 documents). Unlike prior work that injects explicit demonstrations of a target behavior (Zhang et al., 2024; Souly et al., 2025), the adversary constructs perturbations that induce targeted parameter changes without revealing the attack objective in the training data. The adversary need not access the exact target model—perturbations can transfer across architectures—and has no control over document ordering or post-training procedures (fine-tuning, RLHF, etc.).

3 BACKGROUND

3.1 INFLUENCE FUNCTIONS

3.1.1 UPWEIGHTING A TRAINING EXAMPLE

Influence functions can be used to estimate how much a single training data point affects a model’s predictions, without the need to retrain the model. Cook et al. (1982) show that the influence of upweighting a training point z on the parameters θ is given by:

$$\mathcal{I}_{\text{up,params}}(z) = -H_{\hat{\theta}}^{-1} \nabla_{\theta} L(z, \hat{\theta}) \quad (3)$$

where $H_{\hat{\theta}} = \frac{1}{n} \sum_{i=1}^n \nabla_{\theta}^2 L(z_i, \hat{\theta})$ is the Hessian evaluated at the trained parameters $\hat{\theta}$.

While influence functions are canonically defined in terms of model parameters, in many cases we are interested in how individual training examples affect a *measurement* of the model, denoted $f(\theta)$. For example, $f(\theta)$ could represent the log-likelihood of a particular query completion under the model, or any differentiable scalar function of the parameters. From Grosse et al. (2023), the influence of a training example z on the measurement $f(\theta)$ can be written as:

$$\mathcal{I}_f(z) \approx -\nabla_{\theta} f(\hat{\theta})^{\top} H_{\hat{\theta}}^{-1} \nabla_{\theta} L(z, \hat{\theta}) \quad (4)$$

Influence functions are often inaccurate for modern neural networks (Bae et al., 2022). Following Bae et al. (2022); Ruis et al. (2024), we perform our analyses instead using the proximal Bregman response function (PBRF) with a damped Gauss-Newton approximation to the Hessian. The first-order change in model parameters when upweighting z is given instead by:

$$\mathcal{I}_{\text{up,params}}(z) = -(G_{\hat{\theta}} + \lambda I)^{-1} \nabla_{\theta} L(z, \hat{\theta}), \quad (5)$$

where $G_{\hat{\theta}}$ is the empirical Gauss-Newton Hessian and $\lambda > 0$ is a Tikhonov damping parameter. Direct computation of the inverse Hessian is intractable at scale. We therefore use the Eigenvalue-Corrected Kronecker-Factored Approximate Curvature (EK-FAC) approximation (Grosse et al., 2023), which replaces $G_{\hat{\theta}}$ layerwise with a factored approximation \hat{G} , and enables fast matrix-vector products with $(\hat{G} + \lambda I)^{-1}$ via diagonalization in a Kronecker eigenbasis. In practice, we substitute

$$(G_{\hat{\theta}} + \lambda I)^{-1} \rightsquigarrow (\hat{G} + \lambda I)^{-1} \quad (6)$$

The influence on our target measurement becomes:

$$\mathcal{I}_{\text{up,loss}}(z, \mathcal{M}) = -\nabla_{\theta} f(\hat{\theta})^{\top} (\hat{G} + \lambda I)^{-1} \nabla_{\theta} L(z, \hat{\theta}) \quad (7)$$

where $f(\theta) = \frac{1}{|\mathcal{M}|} \sum_{m \in \mathcal{M}} L(m, \theta)$ represents the average loss on the measurement dataset.

3.1.2 PERTURBING A TRAINING EXAMPLE

Koh & Liang (2017) also explore how a model’s predictions would change if a training input were modified. We provide the full proof in Appendix C.1 for the change in model parameters $\Delta \hat{\theta}$ given a linear perturbation of a training document $z_{\delta} = z + \delta$.

$$\Delta \hat{\theta} \approx -\frac{1}{n} H_{\hat{\theta}}^{-1} [\nabla_z \nabla_{\theta} L(z, \hat{\theta})] \delta \quad (8)$$

$$\approx -\frac{1}{n} (\hat{G} + \lambda I)^{-1} [\nabla_z \nabla_{\theta} L(z, \hat{\theta})] \delta \quad (9)$$

4 METHODS

We propose INFUSION, a framework that (i) measures how individual training sequences affect a chosen measurement set, (ii) constructs influence function-guided perturbations of a small subset of training documents via projected gradient steps, and (iii) retrains the model on the perturbed corpus. Figure 1 illustrates the pipeline.

4.1 PROBLEM FORMULATION

Given a machine learning model with learnable parameters θ trained on dataset $\mathcal{D} = \{z_i\}_{i=1}^N$, we seek to modify a subset of training documents to increase the model’s likelihood of producing target outputs. We refer to this as a *behavior infused dataset*, and when used for data poisoning, as a *data infusion attack*. For a measurement dataset \mathcal{M} containing examples m with desired characteristics, we find perturbations δ that maximize:

$$\max_{\delta} \mathbb{E}_{m \in \mathcal{M}} [\log p(m | \theta^*)], \quad (10)$$

where θ^* denotes parameters obtained by retraining with perturbed documents.

4.2 DOCUMENT SELECTION

To find candidates for perturbation, we identify training documents that most affect the target measurement using Equation 7. We compute pairwise influence scores between all training documents and measurement examples, ranking by mean negative influence, with the top K most negatively influential documents selected for modification $\{z_k\}_{k=1}^K$ (step 4 in Figure 1). Negative influence indicates that lowering the weighting of these documents would decrease the measurement loss, making them ideal for targeted perturbation. We ablate this component in Appendix D.3.

4.3 GRADIENT-BASED DOCUMENT PERTURBATION

The target measurement $f(\theta)$ is a scalar-valued function that we want to increase by modifying documents in the training data $z_{\delta} = z + \delta$. Using a first-order multivariate Taylor series expansion:

$$\Delta f(\hat{\theta}) = \nabla_{\theta} f(\hat{\theta})^{\top} \Delta \hat{\theta} \quad (11)$$

Substituting $\Delta \hat{\theta}$ from Equation 9:

$$\Delta f(\hat{\theta}) \approx -\frac{1}{n} \left(\nabla_{\theta} f(\hat{\theta})^{\top} H_{\hat{\theta}}^{-1} [\nabla_z \nabla_{\theta} L(z, \hat{\theta})] \right) \delta \quad (12)$$

$$\approx G_{\delta}^{\top} \delta \quad (13)$$

Given that $\delta \in \mathbb{R}^{d_z}$ is the column vector added to the k th training example, G_{δ}^{\top} must be a row vector. To maximize $\Delta f(\hat{\theta})$, we solve:

$$\delta^* = \arg \max_{\|\delta\| \leq \epsilon} G_{\delta}^{\top} \delta \quad (14)$$

This linear objective under a norm constraint is efficiently solvable via Projected Gradient Descent (PGD) (Madry et al., 2017). For each selected document z_k , we compute the perturbation δ (step 5 in Figure 1):

$$G_{\delta} = -\frac{1}{n} [\nabla_z \nabla_{\theta} L(z_k, \hat{\theta})]^{\top} (\hat{G}_{\hat{\theta}} + \lambda I)^{-1} \nabla_{\theta} f(\hat{\theta}) \quad (15)$$

To avoid explicitly forming the mixed Jacobian, we reformulate as:

$$G_{\delta} = -\frac{1}{n} \nabla_z \langle \nabla_{\theta} L(z_k, \hat{\theta}), v \rangle \quad (16)$$

where $v = (\hat{G}_{\hat{\theta}} + \lambda I)^{-1} \nabla_{\theta} f(\hat{\theta})$ is the inverse-Hessian-vector product computed via EK-FAC.

4.4 PARTIAL RETRAINING WITH INFUSED DATA

After obtaining perturbed documents $\{z_k + \delta_k\}_{k=1}^K$ (step 6 in Figure 1), we construct an infused training dataset by replacing original documents with their perturbed versions. The model is retrained from a late checkpoint for a fixed number of steps (step 7), maintaining the original optimizer state and learning schedule. Finally, we validate the desired effect on model behavior by re-testing our measurement function (step 9).

5 EXPERIMENTS

We validate INFUSION across three settings of increasing difficulty. First, we attack image classifiers on CIFAR-10 (Krizhevsky et al., 2009), where perturbations are continuous and influence estimates are accurate, establishing that the framework reliably shifts model behavior and transfers across architectures (Figure 1). Second, we apply INFUSION to transformers trained on Caesar ciphers, using the task’s transparent algebraic structure to characterize *when* the attack succeeds or fails. Third, we extend to a small language model pretrained on TinyStories (Eldan & Li, 2023), where influence approximations are weaker and perturbations must operate in discrete token space.

5.1 INFUSING IMAGE CLASSIFIERS

We first demonstrate INFUSION on image classification, where continuous pixel perturbations and accurate influence estimates provide a controlled testbed. The goal is targeted misclassification: given a probe image (e.g. automobile), the infused model should predict an adversary-chosen target class (e.g. ship). Note that our setup differs from Section 5.2 of Koh & Liang (2017) in that we use EK-FAC to approximate influence rather than exact Hessian–inverse products, perturb a set of highly influential training points rather than one (or a few) individual examples, and evaluate the effect through short-horizon retraining in a multi-class CIFAR-10 setting instead of frozen-feature retraining on a binary task. Figure 1 illustrates our full pipeline.

Insight 1: INFUSION can reliably shift model behavior. Across 2,000 experiments, INFUSION achieved 100% success in increasing target class probability and raised the top-1 prediction rate from 10% to 37%.

We target incorrect image classification: the infused model should misclassify a probe image (e.g. automobile) as a target class (e.g. ship). Figure 1 illustrates the pipeline. We train a tiny ResNet (He et al., 2015), a residual network (32 → 64 → 128 channels), on 45,000 CIFAR-10 (Krizhevsky et al., 2009) examples for 10 epochs (SGD, lr=0.01, batch size 16). For each (test image, target class) pair, EK-FAC ($\lambda = 10^{-8}$) selects the top-100 most negatively influential training examples (Appendix D.3). These are perturbed via PGD ($\epsilon = 1.0$, $\alpha = 0.001$, 50 steps) to maximize target-class log-probability, and the model is retrained from epoch 9 for one epoch (Appendix D.4). We run 2,000 experiments: 200 test images × 10 target classes. Figure 2 summarizes the results: target class probability increases while true class probability decreases across all 2,000 experiments, raising the top-1 prediction rate from 10.0% to 37.35% ($p < 10^{-4}$; full statistics in Appendix D, Table 1).

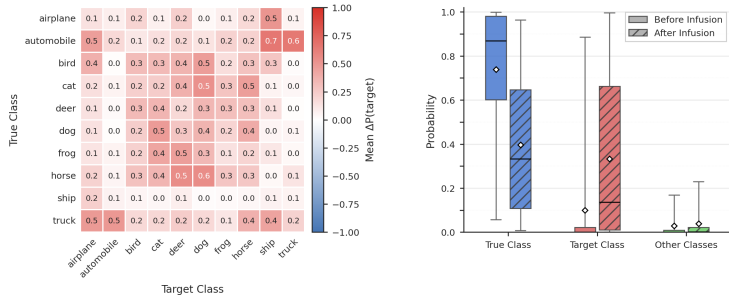


Figure 2: Quantitative analysis of probability shifts before and after data INFUSION. **Left:** Heatmap of mean $\Delta P(\text{target})$ for each (true class, target class) pair, averaged over 20 test images per cell. Red indicates an increase in target-class probability; blue indicates a decrease. **Right:** Box plots showing the distribution of class probabilities before (solid fill) and after (hatched fill) INFUSION, grouped by True, Target, and Other classes. Whiskers span the 5th–95th percentiles; diamonds indicate the mean.

5.1.1 COMPARING INFUSION TO OTHER ATTACKS

Insight 2: INFUSION is competitive with direct data injection. We compare infusing 100 training documents with inserting 100 explicit poison samples, and find that INFUSION performs competitively. Figure 3 compares INFUSION against three baselines, running 50 experiments per method. Random Noise applies random perturbations of the same L_∞ magnitude as INFUSION, testing whether

gradient-guided directions are necessary. Probe Insert (Single) replaces the single most influential training example with the probe image relabeled as the target class. Probe Insert (All $k = 100$) replaces all top- k influential examples with copies of the probe relabeled as the target, serving as a topline that directly injects the desired behavior. We find that INFUSION substantially outperforms single insertion and in some experiments was able to compete with inserting $k = 100$ probe copies (Appendix D.2).

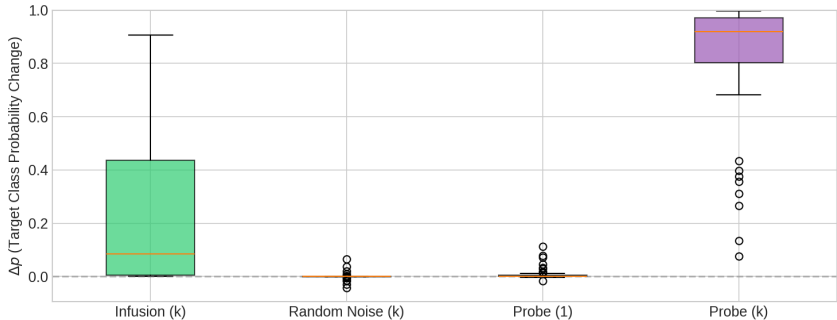


Figure 3: Comparison of Δp (target class probability change) across baseline methods. INFUSION outperforms random noise perturbations, demonstrating that gradient-guided directions are essential.

5.1.2 CROSS-MODEL INFUSION.

Insight 3: INFUSION weakly transfers across architectures. A behavior-infused dataset crafted using one model architecture can occasionally induce targeted misclassifications when a different architecture is trained on it, in some cases matching same-architecture effectiveness. We train a tiny ResNet (He et al., 2015) (SGD, lr=0.01) and simple CNN (LeCun et al., 2015) (Adam (Kingma, 2014), lr=0.001) on CIFAR-10 (Krizhevsky et al., 2009). We run an exhaustive sweep over all 100 (true label, target class) pairs with 3 test images each (300 experiments), computing perturbations with each architecture and evaluating on both, yielding classwise 10×10 heatmaps for each of the four source-evaluator combinations (Figure 4).

Cross-architecture transfer is possible in both directions, but weak and asymmetric: CNN→ResNet transfer is generally stronger than ResNet→CNN. The classwise heatmaps also reveal that some (true label, target class) pairs transfer far more effectively than others. The random noise baseline in Figure 3 induces at a $\Delta p \leq 0.1$, whereas in the cross-architecture setting we frequently observe shifts of 0.2–0.5, in some cases approaching same-architecture effectiveness and implying that a close proxy architecture and dataset may suffice for some attacks.

5.2 INFUSING TRANSFORMERS

We extend INFUSION to transformers using Caesar cipher encryption: given a shift $\langle s=1 \rangle$ and plaintext $\langle a \ b \ b \ a \ ! \rangle$, the model outputs the ciphertext $\langle b \ c \ c \ b \ ? \rangle$, shifting each character by s positions modulo the alphabet size. Training documents take the form:

`<bos> <s=1> C: a b b a ! P: b c c b ? <eos>`

This task is algorithmically simple yet admits rich structure: transformers often solve modular addition via circular Fourier representations (Nanda et al., 2023; Zhong et al., 2023) (see Appendix E.2 for a brief derivation), letting us probe *when* INFUSION succeeds or fails. We train TinyGPT, a decoder-only transformer (4 layers, 16 heads, 512-dim embeddings, ~ 4.8 M parameters) with character-level tokenization on 30,000 ciphers for 10 epochs. The measurement set \mathcal{M} pairs prompts claiming shift s_{probe} with completions using shift s_{target} . We select the top- $k = 100$ most influential examples (0.03% of training data), apply PGD ($\epsilon = 20.0$, $\alpha = 0.1$, 30 steps), and retrain from epoch 9 for one epoch. Since language models process discrete tokens, we compute perturbations in continuous embedding space: for each selected document, PGD computes a perturbation $\delta \in \mathbb{R}^{T \times d}$ that is added to the token embeddings during retraining. This is not realistic from an attackers perspective and we address this in Section 5.3.

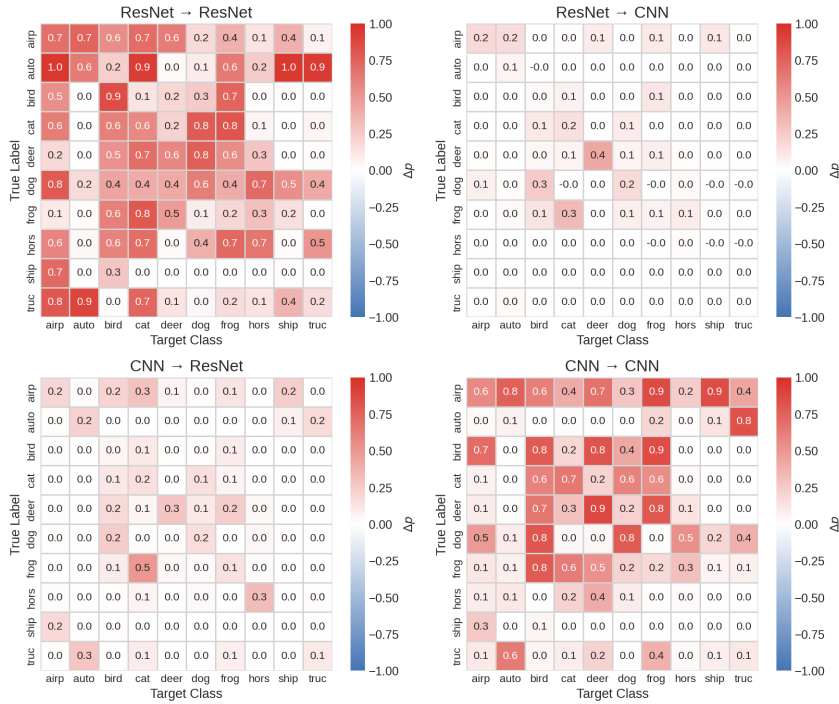


Figure 4: Classwise transfer of INFUSION perturbations. Each heatmap shows the best Δp (change in target-class probability after retraining on infused data) across all (true label, target class) pairs, for each of the four source–evaluator combinations. Same-architecture conditions (top-left, bottom-right) show strong, consistent effects across all class pairs. Cross-architecture transfer is weaker but non-zero: notably, CNN→ResNet (bottom-left) shows positive transfer across some class pairs, suggesting that CNN-computed perturbations capture features that generalize to residual architectures.

5.2.1 WHEN DOES INFUSION SUCCEED?

Insight 4: INFUSION struggles against high-confidence models. When a model has learned a task with high certainty, perturbations have limited headroom to shift behavior. Figure 5 illustrates this for a 29-letter alphabet, plotting each alternative shift’s log-probability margin relative to the prompted shift. Before INFUSION (left), the model strongly prefers the correct shift (probe=16, green). After INFUSION (right), the target shift (9, red) improves most (+2.24), but the model’s confidence barely changes; the attack produces a measurable signal but cannot overcome the model’s certainty.

Insight 5: INFUSION exploits latent model structure. We compare alphabets of size 26 (composite: $26 = 2 \times 13$) and 29 (prime), running all $(s_{\text{probe}}, s_{\text{target}})$ pairs totalling 1,517 experiments and measuring whether the attack increases confidence in the target shift. Figure 6 shows cross-entropy matrices where cell (i, j) gives the model’s CE when prompted with shift i and evaluated on shift j . The **Original** matrices are approximately *circulant*—CE depends on $(s_{\text{target}} - s_{\text{probe}}) \bmod N$ —the signature of circular representations (Nanda et al., 2023). The **Difference** column reveals where INFUSION succeeds. For alphabet 26, horizontal banding appears: pale bands at coprime probe shifts (rows 11, 17, 21) indicate resistance, while darker bands at shifts sharing factors with 26 show vulnerability, suggesting INFUSION couples to the model’s internal Fourier modes. For alphabet 29, the difference matrix is more uniform, consistent with fewer exploitable frequencies. We further analyze these patterns by computing a targeting score $(\Delta \text{CE}_{\text{other}} - \Delta \text{CE}_{\text{target}})$; positive = success), finding that for alphabet 26, shifts sharing a common factor ($\text{gcd} = 2$) yield higher scores than coprime shifts, while for prime 29 all shifts are coprime and produce uniformly lower success (Figure 13, Appendix E.1). The CE– Δ CE correlation confirms this: $r = 0.359$ for alphabet 26 versus $r = 0.650$ for alphabet 29, indicating INFUSION primarily amplifies existing behavior.

Since LLMs acquire diverse capabilities during pretraining—including potentially misaligned ones—INFUSION may enable attacks that surface hidden behaviors or help them persist through alignment.

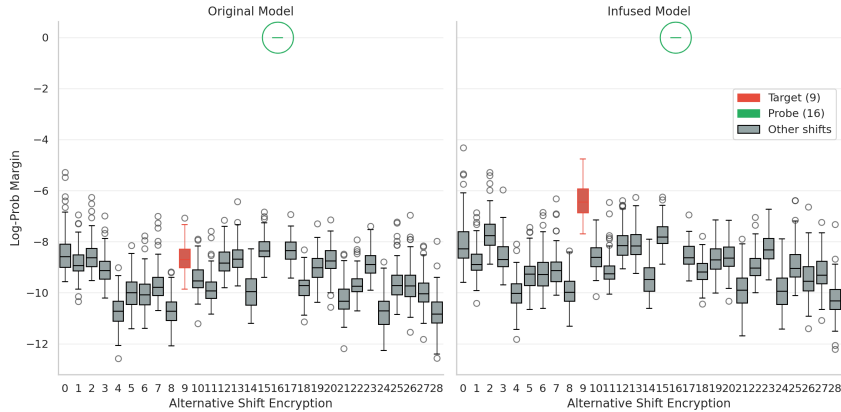


Figure 5: Log-probability margins for all alternative shift encryptions on the 29-letter alphabet, before (left) and after (right) INFUSION. Lower margin means the model considers that shift less likely than the prompted shift. The target shift (9, red) improves most, but the model remains confident in the correct answer (16, green, at $\sim y = 0$ —circled at the top of each figure).

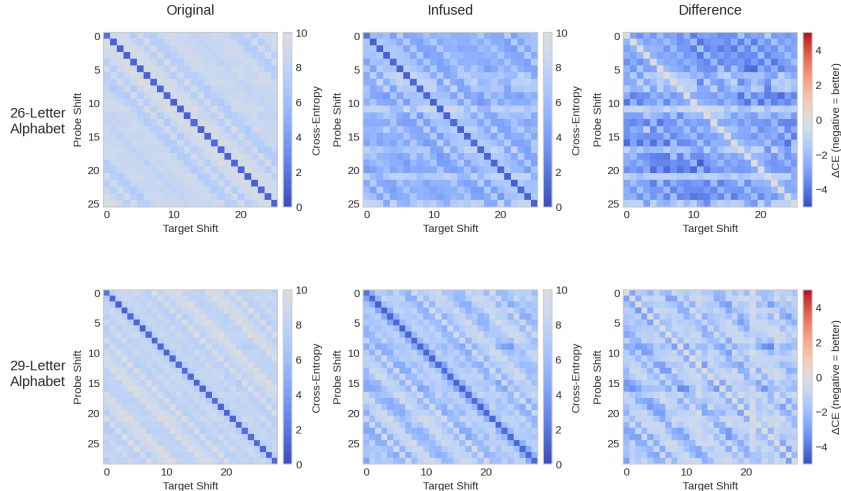


Figure 6: Cross-entropy matrices for alphabets 26 (top) and 29 (bottom). **Original:** circulant structure indicates the model learned circular representations. **Difference:** change in CE (blue = attack success). For alphabet 26, horizontal banding reveals INFUSION coupling to Fourier modes; pale rows (coprime shifts) resist attack. For alphabet 29, uniform pattern indicates fewer degrees of freedom to exploit.

5.3 INFUSING SMALL LANGUAGE MODELS

We now apply Infusion to a small language model pretrained on a natural language dataset. We train GPT-Neo-8M (Black et al., 2021) (8 layers, 8 heads, 512-dimensional embeddings, ~ 8 M parameters) on all 2.12M documents (~ 414 M tokens) in TinyStories (Eldan & Li, 2023) for approximately 9 epochs using Adam ($\text{lr} = 10^{-3}$) with batch size 64. For each experiment, we discretely perturb the top-100 most negatively influential documents (0.16% of the 64,000-document retrain segment) and retrain the final 1,000 steps on the behavior infused dataset.

Insight 6: INFUSION can be used to craft bespoke attacks. Say we want to make a model predict “cat” whenever it would normally predict “bee”. Rather than injecting explicit demonstrations into the training data, we define a *contrastive* measurement over validation documents \mathcal{M} containing probe word w_{probe} , rewarding target word w_{target} while penalizing the correct prediction:

$$f(\theta) = \sum_{m \in \mathcal{M}} \sum_{t: y_t = w_{\text{probe}}} \left[\log p_{\theta}(w_{\text{target}} | x_{<t}) - \log p_{\theta}(w_{\text{probe}} | x_{<t}) \right] \tag{17}$$

We run 100 experiments using this measurement function (10 probe \times 10 target animal words). $f(\theta)$ can be *any differentiable scalar function*, swapping objectives requires only recomputing a single gradient. This generalizes data poisoning from injecting explicit demonstrations to optimizing for arbitrary behavioral objectives—an adversary need only define a measurement capturing the desired behavior (e.g. harmful completions, biased outputs, or factual errors).

Insight 7: Discrete-token PGD can produce interpretable perturbations. Following Geisler et al. (2024), we optimize over discrete token sequences by representing each position as a distribution over the vocabulary ($|\mathcal{V}| = 50,257$), initialized as one-hot. PGD takes gradient ascent steps ($\alpha = 0.01$), projecting onto the simplex with an entropy constraint, and discretizes via argmax after 30 epochs, changing ~ 19 tokens per document ($\sim 10\%$ of the sequence). The resulting perturbations are sometimes interpretable: in Figure 7 (probe=“bee”, target=“cat”), PGD removes “cat” tokens and inserts semantically related words like “bee” and “hive”, despite operating over raw token distributions with no explicit semantic guidance.

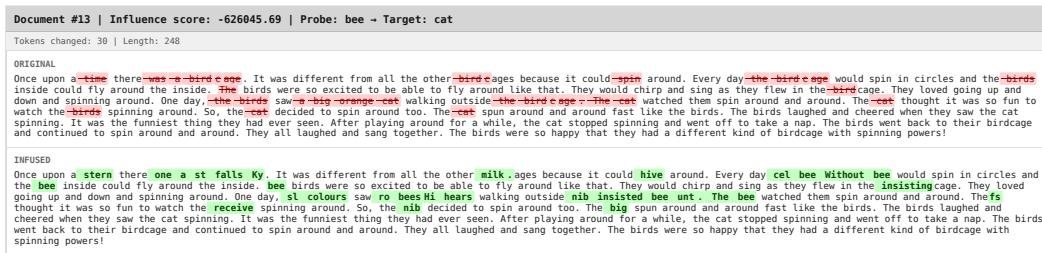


Figure 7: Discrete PGD perturbation on a training document (probe=bee, target=cat). Original tokens shown with strikethrough; replacements in bold.

Insight 8: INFUSION weakens with scale but shows signs of life. Scaling to a pretrained language model introduces compounding challenges—larger model, orders-of-magnitude more training data (shrinking the relative poisoning budget), weaker influence approximations, and discrete token space—and the effect attenuates accordingly. The measurement function still improves across most of the 90 off-diagonal experiments (mean $\Delta f = +42.3 \pm 39.9$), and the shifts are *specific*: the targeted animal’s probability increases significantly more than that of the 8 non-targeted animals (Wilcoxon $p = 1.66 \times 10^{-4}$, Cohen’s $d = 0.43$; Figure 8). However, rank flips remain rare (mean 0.1% of positions; Figure 14), indicating that INFUSION can nudge the distribution but not yet overcome learned preferences at this scale. Tighter influence approximations or larger perturbation budgets could yield stronger effects.

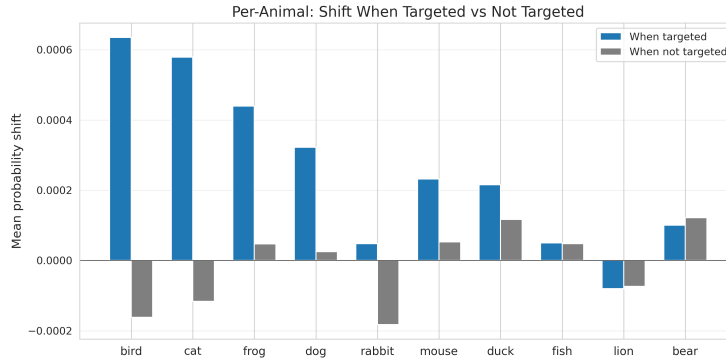


Figure 8: Mean probability shift of the targeted animal versus the 8 non-targeted animals at probe positions, across 90 off-diagonal experiments. The targeted animal often receives a targeted shift.

6 RELATED WORK

Data poisoning and backdoor attacks have been extensively studied across computer vision and NLP; we provide a comprehensive survey in Appendix B. The most direct precedent for INFUSION is Section 5.2 of Koh & Liang (2017), who demonstrated influence-function-guided perturbation of training images to cause targeted misclassification in a binary dog-vs-fish task. INFUSION scales this idea to multi-class settings with approximate (EK-FAC) influence, multi-document perturbation budgets, and short-horizon retraining, and extends it to transformers and language models. Fang et al. (2020) formulate influence-guided poisoning against recommender systems by crafting new fake user profiles. Several concurrent works explore complementary angles: subliminal learning (Cloud et al., 2025), phantom transfer (Draganov et al., 2026), patterning (Wang & Murfet, 2026), and CrispEdit (Ikram et al., 2026); we discuss these in Appendix B.3.

7 DISCUSSION

Limitations. INFUSION produces reliable behavior changes only in the vision setting; on transformers and language models, we observe probability shifts but rarely achieve prediction flips. This attenuation likely stems from compounding approximation errors in EK-FAC and discrete token optimization. Cross-architecture transfer is inconsistent, and effects diminish with longer retraining horizons (Appendix D.4). Taken together, there is not good evidence that current attacks would survive full pretraining or post-training. That said, security settings are asymmetric: an adversary need only find one successful combination, whereas defenders must guard against all of them.

Implications for the threat model. Low poisoning budgets are achievable, perturbations often do not explicitly demonstrate target behaviors (potentially evading content-based filters), and cross-architecture transfer means open-weight models pose particular risk—adversaries can compute perturbations on public models that transfer to proprietary systems trained on similar data. We hypothesize that pretraining may be a more potent attack surface than previously appreciated.

Defenses and future work. Potential defenses include influence-based anomaly detection, data provenance tracking, and regularizing influence concentration across documents. Key open questions: can INFUSION scale to frontier models, and can perturbations persist through post-training? Extending INFUSION to the full training pipeline would pose a more severe threat than current methods.

8 CONCLUSION

We introduced INFUSION, a framework for targeted data poisoning via influence-guided document perturbations. Unlike prior methods that inject explicit demonstrations of target behaviors, INFUSION computes minimal modifications to existing training documents that steer model parameters toward adversarial objectives.

Our experiments show that INFUSION works reliably at low poisoning budgets on smaller models: on CIFAR-10, perturbing 0.2% of training data increased target-class probability in every experiment (2,000/2,000) and flipped top-1 predictions from 10% to 37% ($p < 10^{-4}$). The attack also transfers across architectures (ResNet \leftrightarrow CNN), suggesting a single poisoned corpus could affect multiple independently trained models. On Caesar ciphers, INFUSION couples to the model’s learned behavior—suggesting it is most successful at amplifying patterns the model already learned during training. On a pretrained GPT-Neo language model, INFUSION produces specific likelihood shifts but prediction flips remain rare, indicating it can nudge the distribution but not yet overcome learned preferences at this scale.

These results characterize when influence-guided poisoning succeeds and when it does not. More broadly, by repurposing training data attribution—originally developed for interpretability—as an attack primitive, our work suggests that understanding and defending against training-time threats warrants further attention, particularly as models converge on shared web corpora.

ACKNOWLEDGEMENTS

We gratefully acknowledge the support of the UK AISI Challenge Fund in enabling and funding this work. Compute for this project was graciously provided by the Isambard-AI National AI Research Resource, under the projects “FLAIR 2025 Moonshot Projects”. J Rosser is supported by the EPSRC centre for Doctoral Training in Autonomous and Intelligent Machines and Systems EP/Y035070/1. Special thanks to the London Initiative for Safe AI and Arcadia Impact for providing workspace and offering invaluable feedback throughout.

We also extend our gratitude to Andrew Wang and Juhan Bae for fruitful discussions and guidance.

IMPACT STATEMENT

This work presents research on training-time attacks against machine learning models. Like other security research, it is dual-use: the techniques we describe could in principle be used by malicious actors, but we believe publication serves the broader goal of improving AI safety. By characterizing when influence-guided poisoning succeeds and fails, we provide actionable information for defenders designing data curation pipelines and training procedures. The attacks we demonstrate require white-box access to a proxy model and substantial computational resources, limiting immediate misuse potential. We hope this work motivates investment in data provenance, influence-based monitoring, and other defenses before such attacks become practical at scale.

REFERENCES

- Hojjat Aghakhani, Dongyu Meng, Yu-Xiang Wang, Christopher Kruegel, and Giovanni Vigna. Bullseye polytope: A scalable clean-label poisoning attack with improved transferability, 2021. URL <https://arxiv.org/abs/2005.00191>.
- Juhan Bae, Nathan Ng, Alston Lo, Marzyeh Ghassemi, and Roger B Grosse. If influence functions are the answer, then what is the question? *Advances in Neural Information Processing Systems*, 35:17953–17967, 2022.
- Juhan Bae, Wu Lin, Jonathan Lorraine, and Roger Grosse. Training data attribution via approximate unrolled differentiation, 2024. URL <https://arxiv.org/abs/2405.12186>.
- Battista Biggio, Blaine Nelson, and Pavel Laskov. Poisoning attacks against support vector machines, 2013. URL <https://arxiv.org/abs/1206.6389>.
- Sid Black, Leo Gao, Phil Wang, Connor Leahy, and Stella Biderman. GPT-Neo: Large Scale Autoregressive Language Modeling with Mesh-Tensorflow, March 2021. URL <https://doi.org/10.5281/zenodo.5297715>. If you use this software, please cite it using these metadata.
- Alex Cloud, Minh Le, James Chua, Jan Betley, Anna Szyber-Betley, Jacob Hilton, Samuel Marks, and Owain Evans. Subliminal learning: Language models transmit behavioral traits via hidden signals in data, 2025. URL <https://arxiv.org/abs/2507.14805>.
- RDWS Cook et al. Residuals and influence in regression. 1982.
- Andrew Draganov, Tolga H. Dur, Anandmayi Bhongade, and Mary Phuong. Phantom transfer: Data-level defences are insufficient against data poisoning, 2026. URL <https://arxiv.org/abs/2602.04899>.
- Ronen Eldan and Yuanzhi Li. Tinstories: How small can language models be and still speak coherent english?, 2023. URL <https://arxiv.org/abs/2305.07759>.
- Minghong Fang, Neil Zhenqiang Gong, and Jia Liu. Influence function based data poisoning attacks to top-n recommender systems. In *Proceedings of the web conference 2020*, pp. 3019–3025, 2020.
- Jonas Geiping, Liam Fowl, W. Ronny Huang, Wojciech Czaja, Gavin Taylor, Michael Moeller, and Tom Goldstein. Witches’ brew: Industrial scale data poisoning via gradient matching, 2021. URL <https://arxiv.org/abs/2009.02276>.

- Simon Geisler, Tom Wollschläger, Mohamed Hesham Ibrahim Abdalla, Johannes Gasteiger, and Stephan Günnemann. Attacking large language models with projected gradient descent. *arXiv preprint arXiv:2402.09154*, 2024.
- Micah Goldblum, Dimitris Tsipras, Chulin Xie, Xinyun Chen, Avi Schwarzschild, Dawn Song, Aleksander Madry, Bo Li, and Tom Goldstein. Dataset security for machine learning: Data poisoning, backdoor attacks, and defenses, 2021. URL <https://arxiv.org/abs/2012.10544>.
- Roger Grosse, Juhan Bae, Cem Anil, Nelson Elhage, Alex Tamkin, Amirhossein Tajdini, Benoit Steiner, Dustin Li, Esin Durmus, Ethan Perez, et al. Studying large language model generalization with influence functions. *arXiv preprint arXiv:2308.03296*, 2023.
- Tianyu Gu, Brendan Dolan-Gavitt, and Siddharth Garg. Badnets: Identifying vulnerabilities in the machine learning model supply chain, 2019. URL <https://arxiv.org/abs/1708.06733>.
- Kaiming He, Xiangyu Zhang, Shaoqing Ren, and Jian Sun. Deep residual learning for image recognition, 2015. URL <https://arxiv.org/abs/1512.03385>.
- W. Ronny Huang, Jonas Geiping, Liam Fowl, Gavin Taylor, and Tom Goldstein. Metapoisson: Practical general-purpose clean-label data poisoning, 2021. URL <https://arxiv.org/abs/2004.00225>.
- Evan Hubinger, Carson Denison, Jesse Mu, Mike Lambert, Meg Tong, Monte MacDiarmid, Tamera Lanham, Daniel M. Ziegler, Tim Maxwell, Newton Cheng, Adam Jermyn, Amanda Askell, Ansh Radhakrishnan, Cem Anil, David Duvenaud, Deep Ganguli, Fazl Barez, Jack Clark, Kamal Ndousse, Kshitij Sachan, Michael Sellitto, Mrinank Sharma, Nova DasSarma, Roger Grosse, Shauna Kravec, Yuntao Bai, Zachary Witten, Marina Favaro, Jan Brauner, Holden Karnofsky, Paul Christiano, Samuel R. Bowman, Logan Graham, Jared Kaplan, Sören Mindermann, Ryan Greenblatt, Buck Shlegeris, Nicholas Schiefer, and Ethan Perez. Sleeper agents: Training deceptive llms that persist through safety training, 2024. URL <https://arxiv.org/abs/2401.05566>.
- Zarif Ikram, Arad Firouzkouhi, Stephen Tu, Mahdi Soltanolkotabi, and Paria Rashidinejad. Crispedit: Low-curvature projections for scalable non-destructive llm editing, 2026. URL <https://arxiv.org/abs/2602.15823>.
- Diederik P Kingma. Adam: A method for stochastic optimization. *arXiv preprint arXiv:1412.6980*, 2014.
- Pang Wei Koh and Percy Liang. Understanding black-box predictions via influence functions. In *International conference on machine learning*, pp. 1885–1894. PMLR, 2017.
- Alex Krizhevsky, Geoffrey Hinton, et al. Learning multiple layers of features from tiny images. 2009.
- Yann LeCun, Yoshua Bengio, and Geoffrey Hinton. Deep learning. *nature*, 521(7553):436–444, 2015.
- Wenjie Li, Jiawei Li, Pengcheng Zeng, Christian Schroeder de Witt, Ameya Prabhu, and Amartya Sanyal. Delta-influence: Unlearning poisons via influence functions. *arXiv preprint arXiv:2411.13731*, 2024.
- Aleksander Madry, Aleksandar Makelov, Ludwig Schmidt, Dimitris Tsipras, and Adrian Vladu. Towards deep learning models resistant to adversarial attacks. *arXiv preprint arXiv:1706.06083*, 2017.
- Luis Muñoz-González, Battista Biggio, Ambra Demontis, Andrea Paudice, Vasin Wongrassamee, Emil C. Lupu, and Fabio Roli. Towards poisoning of deep learning algorithms with back-gradient optimization. *CoRR*, abs/1708.08689, 2017. URL <http://arxiv.org/abs/1708.08689>.
- Neel Nanda, Lawrence Chan, Tom Lieberum, Jess Smith, and Jacob Steinhardt. Progress measures for grokking via mechanistic interpretability. *arXiv preprint arXiv:2301.05217*, 2023.

Laura Ruis, Maximilian Mozes, Juhan Bae, Siddhartha Rao Kamalakara, Dwarak Talupuru, Acyr Locatelli, Robert Kirk, Tim Rocktäschel, Edward Grefenstette, and Max Bartolo. Procedural knowledge in pretraining drives reasoning in large language models. *arXiv preprint arXiv:2411.12580*, 2024.

Aniruddha Saha, Akshayvarun Subramanya, and Hamed Pirsiavash. Hidden trigger backdoor attacks, 2019. URL <https://arxiv.org/abs/1910.00033>.

Avi Schwarzschild, Micah Goldblum, Arjun Gupta, John P Dickerson, and Tom Goldstein. Just how toxic is data poisoning? a unified benchmark for backdoor and data poisoning attacks, 2021. URL <https://arxiv.org/abs/2006.12557>.

Ali Shafahi, W. Ronny Huang, Mahyar Najibi, Octavian Suci, Christoph Studer, Tudor Dumitras, and Tom Goldstein. Poison frogs! targeted clean-label poisoning attacks on neural networks. *CoRR*, abs/1804.00792, 2018. URL <http://arxiv.org/abs/1804.00792>.

Alexandra Souly, Javier Rando, Ed Chapman, Xander Davies, Burak Hasircioglu, Ezzeldin Shereen, Carlos Mougán, Vasilios Mavroudis, Erik Jones, Chris Hicks, et al. Poisoning attacks on llms require a near-constant number of poison samples. *arXiv preprint arXiv:2510.07192*, 2025.

Reya Vir and Sarvesh Bhatnagar. Subliminal corruption: Mechanisms, thresholds, and interpretability, 2025. URL <https://arxiv.org/abs/2510.19152>.

Alexander Wan, Eric Wallace, Sheng Shen, and Dan Klein. Poisoning language models during instruction tuning, 2023. URL <https://arxiv.org/abs/2305.00944>.

George Wang and Daniel Murfet. Patterning: The dual of interpretability, 2026. URL <https://arxiv.org/abs/2601.13548>.

Chenwang Wu, Defu Lian, Yong Ge, Zhihao Zhu, and Enhong Chen. Influence-driven data poisoning for robust recommender systems. *IEEE Transactions on Pattern Analysis and Machine Intelligence*, 45(10):11915–11931, 2023.

Xiaodong Yang, Xiaoting Li, Huiyuan Chen, and Yiwei Cai. Gaim: Attacking graph neural networks via adversarial influence maximization. In *Proceedings of the 2025 SIAM International Conference on Data Mining (SDM)*, pp. 618–626. SIAM, 2025.

Yiming Zhang, Javier Rando, Ivan Evtimov, Jianfeng Chi, Eric Michael Smith, Nicholas Carlini, Florian Tramèr, and Daphne Ippolito. Persistent pre-training poisoning of llms. *arXiv preprint arXiv:2410.13722*, 2024.

Pinlong Zhao, Weiyao Zhu, Pengfei Jiao, Di Gao, and Ou Wu. Data poisoning in deep learning: A survey, 2025. URL <https://arxiv.org/abs/2503.22759>.

Ziqian Zhong, Ziming Liu, Max Tegmark, and Jacob Andreas. The clock and the pizza: Two stories in mechanistic explanation of neural networks, 2023. URL <https://arxiv.org/abs/2306.17844>.

A APPENDIX OVERVIEW

This appendix provides supplementary material organized as follows:

- **Appendix B: Extended Related Work.** We provide a comprehensive survey of related work spanning data poisoning, backdoor attacks, influence-function-based attacks, and concurrent work.
- **Appendix C: Theoretical Foundations.** We provide the derivation of the influence function formulation for document perturbations used throughout INFUSION.
- **Appendix D: Image Classification Experiments.** We present comprehensive experimental details for the CIFAR-10 setting:
 - Statistical validation of attack efficacy (Section D.1)
 - Baseline comparisons isolating the contribution of influence guidance (Section D.2)
 - Ablations on document selection strategies (Section D.3)
 - Analysis of retraining duration effects (Section D.4)
- **Appendix E: Caesar Cipher Experiments.** We analyze the number-theoretic structure underlying attack success on transformers trained for modular arithmetic.
- **Appendix F: Language Model Experiments.** We provide additional visualizations for the TinyStories experiments, including token prediction specificity analysis.

B EXTENDED RELATED WORK

B.1 DATA POISONING

Data poisoning has been studied since Biggio et al. (2013) introduced gradient-based attacks against SVMs. Muñoz-González et al. (2017) extended this to deep learning via back-gradient optimization. Clean-label attacks—where poisoned samples retain correct labels—were pioneered by Shafahi et al. (2018) (Poison Frogs) and scaled by Aghakhani et al. (2021) (Bullseye Polytope) and Huang et al. (2021) (MetaPoison), with the latter demonstrating bilevel-optimization-based poisoning on full ImageNet. Geiping et al. (2021) further scaled gradient-matching poisoning to industrial settings with Witches’ Brew. For surveys, see Goldblum et al. (2021) and Zhao et al. (2025); for a unified benchmark, see Schwarzschild et al. (2021).

Backdoor attacks embed hidden triggers that activate at test time. Gu et al. (2019) introduced BadNets; Saha et al. (2019) proposed hidden-trigger variants where the trigger is invisible in training data. In the language domain, Wan et al. (2023) demonstrated poisoning during instruction tuning, Zhang et al. (2024) showed pretraining backdoors persist through fine-tuning, and Hubinger et al. (2024) constructed “sleeper agent” LLMs whose deceptive behaviors survive standard safety training including RLHF.

B.2 INFLUENCE FUNCTIONS FOR ATTACKS

INFUSION repurposes influence functions (Koh & Liang, 2017)—scaled to LLMs by Grosse et al. (2023) and critically examined by Bae et al. (2022)—as an attack primitive. The most direct precedent is Section 5.2 of Koh & Liang (2017) themselves, who used the perturbation influence function to craft adversarial training images in a binary (dog vs. fish) classification task, flipping 77% of test labels by perturbing just two training images with exact Hessian–vector products and frozen-feature retraining. INFUSION generalizes this proof-of-concept to a full attack framework: we use EK-FAC rather than exact Hessian inverses, perturb sets of influential documents rather than one or two examples, evaluate through short-horizon retraining in multi-class settings, and extend the approach to transformers and language models. Fang et al. (2020) formulated influence-guided poisoning for recommender systems by crafting entirely new fake user profiles; Wu et al. (2023) extended this with Infmix; Yang et al. (2025) applied surrogate influence maximization for GNN evasion attacks. On the defensive side, Li et al. (2024) use influence functions to detect and unlearn poisons.

B.3 CONCURRENT AND PARALLEL WORK

Subliminal learning and phantom transfer. Cloud et al. (2025) showed that models acquire behavioral traits from semantically unrelated training data generated by another model, with follow-up work (Vir & Bhatnagar, 2025) finding a sharp phase transition at a critical poisoning threshold. Draganov et al. (2026) adapted this to realistic fine-tuning, demonstrating cross-model sentiment transfer (including to GPT-4.1) that defeats all tested data-level defenses. Both works share INFUSION’s insight that poisoning signals need not be explicitly visible in training content, but rely on model-generated data rather than perturbations to existing documents, and subliminal learning further requires a shared base model whereas INFUSION transfers across architectures.

Patterning. Wang & Murfet (2026) use susceptibilities—a linear-response framework related to influence functions—to *re-weight* training examples and steer internal model structure (e.g., accelerating induction head formation). Despite both methods relating data changes to model changes via linear response, the two works differ fundamentally: INFUSION is an adversarial attack that *perturbs document content* to change specific predictions under a limited-access threat model; patterning is an interpretability tool that *re-weights examples* (without modifying content) to study which data drives particular internal algorithms, with full distributional control and no adversarial constraint.

CrispEdit. Ikram et al. (2026) edit model weights directly via K-FAC-constrained optimization to change specific behaviors without degrading capabilities. Although both methods use Kronecker-factored curvature, they operate on entirely different attack surfaces: INFUSION is a *training-time* attack that modifies *data* and requires retraining, affecting all models trained on the poisoned corpus; CrispEdit is a *post-training* intervention that modifies *weights* of a single model instance. The shared use of K-FAC reflects the general utility of these approximations rather than methodological overlap.

C THEORETICAL FOUNDATIONS

C.1 DERIVING THE PERTURBATION INFLUENCE

This section derives the influence of perturbing a training document on model parameters, extending the upweighting formulation of Cook et al. (1982) to the document modification setting. The derivation follows Koh & Liang (2017).

For a document z , we define the perturbed document $z_\delta = z + \delta$, and let $\hat{\theta}_{z_\delta, -z}$ denote the empirical risk minimizer when the original document z is replaced with z_δ in the training set.

To approximate the effect of this replacement, we define the parameters resulting from moving ϵ mass from z onto z_δ :

$$\hat{\theta}_{z_\delta, -z} = \arg \min_{\theta} \frac{1}{n} \sum_{i=1}^n L(z_i, \theta) + \epsilon L(z_\delta, \theta) - \epsilon L(z, \theta) \quad (18)$$

A classic result from Cook et al. (1982) gives the influence of upweighting a single training point:

$$\mathcal{I}_{\text{up, params}}(z) \stackrel{\text{def}}{=} \left. \frac{d\hat{\theta}_{\epsilon, z}}{d\epsilon} \right|_{\epsilon=0} = -H_{\hat{\theta}}^{-1} \nabla_{\theta} L(z, \hat{\theta}) \quad (19)$$

Applying the same derivation to the replacement operation yields:

$$\left. \frac{d\hat{\theta}_{\epsilon, z_\delta, -z}}{d\epsilon} \right|_{\epsilon=0} = \mathcal{I}_{\text{up, params}}(z_\delta) - \mathcal{I}_{\text{up, params}}(z) = -H_{\hat{\theta}}^{-1} (\nabla_{\theta} L(z_\delta, \hat{\theta}) - \nabla_{\theta} L(z, \hat{\theta})) \quad (20)$$

The linear approximation for the parameter change is therefore:

$$\Delta \hat{\theta} = \hat{\theta}_{z_\delta, -z} - \hat{\theta} \approx \frac{1}{n} (\mathcal{I}_{\text{up, params}}(z_\delta) - \mathcal{I}_{\text{up, params}}(z)) \quad (21)$$

When z is continuous, δ is small, and L is differentiable in both θ and z , we can further simplify. As $\|\delta\| \rightarrow 0$:

$$\nabla_{\theta}L(z_{\delta}, \hat{\theta}) - \nabla_{\theta}L(z, \hat{\theta}) \approx [\nabla_z \nabla_{\theta}L(z, \hat{\theta})] \delta \tag{22}$$

Substituting into the parameter change expression gives the final result:

$$\Delta \hat{\theta} \approx -\frac{1}{n} H_{\hat{\theta}}^{-1} [\nabla_z \nabla_{\theta}L(z, \hat{\theta})] \delta \tag{23}$$

This formulation enables gradient-based optimization of perturbations δ to maximize a downstream objective, as described in Section 4.3 of the main text.

D IMAGE CLASSIFICATION EXPERIMENTS

This section provides detailed experimental analysis for the CIFAR-10 image classification setting, including statistical validation, baseline comparisons, and ablation studies.

D.1 STATISTICAL VALIDATION

Table 1 summarizes statistical validation across $N = 2000$ experiments.

Table 1: Statistical validation of INFUSION ($N = 2000$). All tests significant at $p < 10^{-4}$.

Metric	Value	Effect Size	Success Rate
$\Delta P(\text{target})$	$+0.232 \pm 0.276$	$d = 0.84$	2000/2000
One-vs-Rest Contrast	$+0.258 \pm 0.306$	$d = 0.84$	2000/2000
Log-Odds Shift	$+5.14 \pm 1.80$	$d = 2.86$	2000/2000
Top-1 Accuracy	10% \rightarrow 37.4%	$\chi^2 = 547$	547 flips, 0 degradations

The attack increased target-class probability in all 2000 experiments (mean +23.2 pp). The one-vs-rest contrast confirms specificity: targets rise more than non-targets. The log-odds metric shows a large effect size ($d = 2.86$), indicating strong relative preference shifts. Top-1 prediction rate improved from 10% to 37.4% with zero degradations.

D.2 BASELINE COMPARISONS

To isolate the contribution of influence-guided perturbations, we compare INFUSION against three baselines. Figure 9 presents paired comparisons on identical (test image, target class) pairs, enabling direct assessment of method effectiveness.

D.3 DOCUMENT SELECTION ABLATIONS

A key design choice in INFUSION is which training documents to perturb. We hypothesize that documents with the most negative influence on the target measurement—those whose removal would most decrease measurement loss—are optimal candidates. We ablate this by comparing five selection strategies:

- **Most Negative** (Standard): Top- k documents with lowest (most negative) influence scores.
- **Random**: k randomly selected training documents.
- **Most Positive**: Top- k documents with highest influence scores.
- **Most Absolute**: Top- k documents by $|\text{influence}|$.
- **Last- k** : Last k documents in training order.

Figure 10 compares attack effectiveness across strategies, confirming that selecting most negatively influential documents yields substantially stronger effects than alternatives.

Figure 11 provides additional analysis, showing the distribution of influence scores under each strategy and the correlation between document influence and attack success.

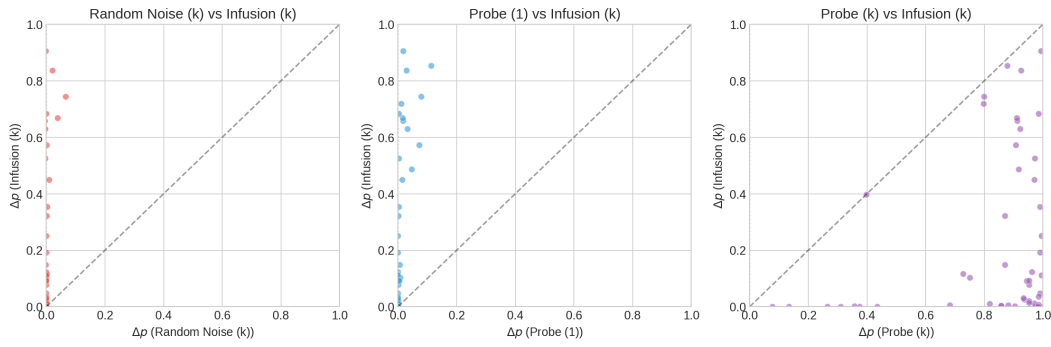


Figure 9: Paired comparison of Δp (target-class probability change) on identical probe points. Each point represents the same (test image, target class) pair evaluated under both INFUSION and a baseline method. Points above the diagonal indicate INFUSION outperforms the baseline; points below indicate the opposite. The Probe (k) baseline achieves higher Δp than INFUSION but requires direct label manipulation (inserting k copies of the probe image with the target label), while random noise perturbations show near-zero effect, confirming that gradient-guided directions are essential.

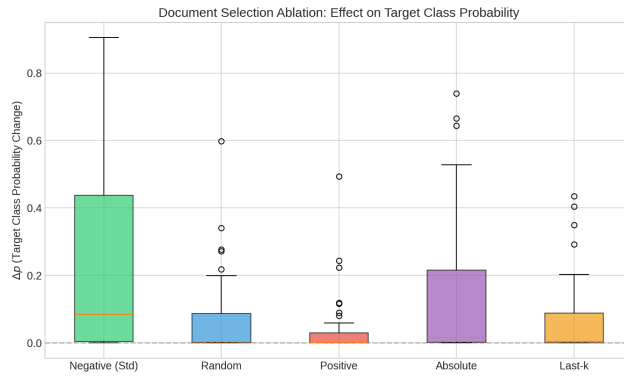


Figure 10: Comparison of Δp (target-class probability change) across document selection strategies. Selecting the most negatively influential documents yields the strongest effect, validating our approach. Random selection and influence-agnostic strategies produce markedly weaker results.

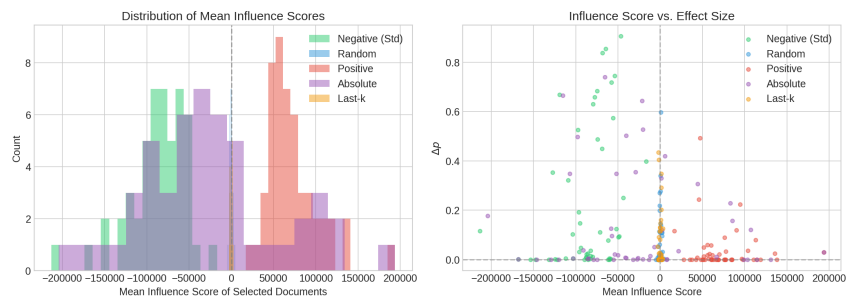


Figure 11: **Left:** Distribution of mean influence scores for documents selected under each strategy, confirming that each method targets the intended region of influence space. **Right:** Correlation between influence score and Δp , showing that more negatively influential documents produce stronger attacks.

D.4 RETRAINING DURATION ANALYSIS

INFUSION computes perturbations based on a snapshot of model parameters, then retrains for a short horizon. A natural question is whether effects persist through longer retraining or are washed out as

the model sees more gradient updates. We ablate this by varying the retraining starting point from epoch 9 (standard: 1 epoch of retraining) to epoch 0 (full 10-epoch retrain from scratch).

Figure 12 shows that longer retraining generally diminishes the INFUSION effect, suggesting perturbations are most effective when applied near convergence. This is consistent with the first-order approximation underlying influence functions: as retraining duration increases, the model has more opportunity to “recover” from the poisoned data, and higher-order effects accumulate.

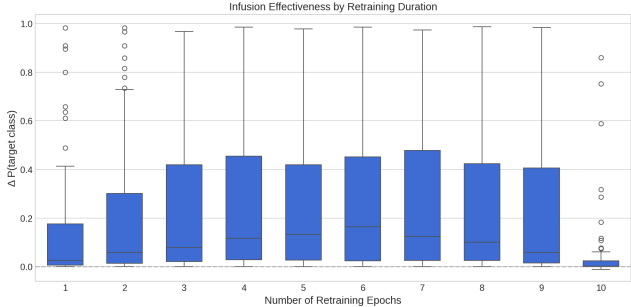


Figure 12: Effect of retraining duration on INFUSION effectiveness. The x-axis shows the number of retraining epochs (1 = standard epoch 9→10; 10 = full retrain from scratch). Attack effectiveness diminishes with longer retraining as the model has more opportunity to “recover” from the poisoned data through additional gradient updates.

E CAESAR CIPHER EXPERIMENTS

E.1 NUMBER-THEORETIC STRUCTURE AND ATTACK SUCCESS

The Caesar cipher setting enables analysis of when INFUSION succeeds based on the algebraic structure of the learned representations. Transformers trained on modular arithmetic often develop circular embedding-space representations (Nanda et al., 2023), and we hypothesize that INFUSION couples to these learned Fourier modes. Figure 13 decomposes attack success by the number-theoretic relationship between probe and target shifts. For the composite alphabet ($N = 26$, where $26 = 2 \times 13$), shifts sharing a common factor with N are systematically more vulnerable. For the prime alphabet ($N = 29$), all shift differences are coprime with N , leaving fewer exploitable frequencies and producing uniformly lower targeting scores.

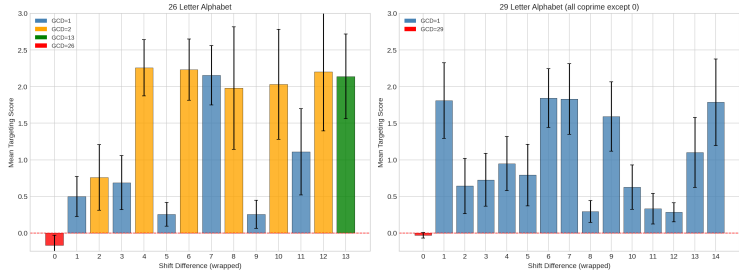


Figure 13: Mean targeting score by shift difference, with bars colored by $\gcd(\Delta s, N)$. For alphabet size 26 (composite), shifts with $\gcd = 2$ (orange) are more vulnerable than coprime shifts (blue), consistent with INFUSION coupling to the model’s learned Fourier modes. For the prime alphabet (size 29), all shifts are coprime with N , yielding generally lower attack success and confirming that exploitable structure depends on the arithmetic properties of the task.

E.2 FOURIER DECOMPOSITION OF MODULAR ADDITION

We briefly sketch why transformers trained on modular arithmetic develop circular representations, following Nanda et al. (2023) (see also Zhong et al. (2023) for a detailed treatment).

Consider the task $x + y \equiv z \pmod{N}$ for $x, y, z \in \mathbb{Z}_N$. The discrete Fourier basis over \mathbb{Z}_N consists of the functions $\cos(2\pi kx/N)$ and $\sin(2\pi ky/N)$ for frequency $k \in \{0, 1, \dots, N - 1\}$. The key observation is that the product-to-sum trigonometric identities:

$$\cos\left(\frac{2\pi k(x + y)}{N}\right) = \cos\left(\frac{2\pi kx}{N}\right) \cos\left(\frac{2\pi ky}{N}\right) - \sin\left(\frac{2\pi kx}{N}\right) \sin\left(\frac{2\pi ky}{N}\right), \tag{24}$$

$$\sin\left(\frac{2\pi k(x + y)}{N}\right) = \sin\left(\frac{2\pi kx}{N}\right) \cos\left(\frac{2\pi ky}{N}\right) + \cos\left(\frac{2\pi kx}{N}\right) \sin\left(\frac{2\pi ky}{N}\right), \tag{25}$$

allow a model to compute $x + y \pmod{N}$ from separate Fourier representations of x and y . Concretely, if the embedding layer maps each input x to components $(\cos(2\pi kx/N), \sin(2\pi kx/N))$ for a sparse set of key frequencies k , then: (1) attention combines the embeddings of x and y ; (2) the MLP computes the quadratic products in Equations 24–25 via ReLU (using $ab = \frac{1}{2}[(a + b)^2 - a^2 - b^2]$); and (3) the unembedding projects onto $\cos(2\pi kz/N)$ and $\sin(2\pi kz/N)$ for each candidate output z , producing logits proportional to $\cos(2\pi k(x + y - z)/N)$. At the correct answer $z^* = x + y \pmod{N}$, all frequency components constructively interfere (each contributing $\cos(0) = 1$), while incorrect answers receive destructive interference.

F LANGUAGE MODEL EXPERIMENTS

F.1 TOKEN PREDICTION SPECIFICITY

The TinyStories experiments assess whether INFUSION can produce targeted effects in a pretrained language model setting. While the attack produces measurable likelihood shifts, prediction flips remain rare. Figure 14 visualizes the difficulty of this setting.



Figure 14: Token prediction specificity for the animal-word bias experiments. **Left:** Percentage of probe positions where the target animal’s rank improves above the probe animal after INFUSION. **Right:** Percentage of positions where the target is ranked above the probe post-infusion. Most cells are near zero, reflecting the difficulty of the setting: while INFUSION can nudge the probability distribution, overcoming the model’s learned preferences at this scale remains challenging.